

Ultrafast Structural Dynamics in InSb Probed by Time-Resolved X-Ray Diffraction

A. H. Chin,^{1,2,*} R. W. Schoenlein,² T. E. Glover,³ P. Balling,⁵ W. P. Leemans,⁴ and C. V. Shank^{1,2}

¹*Department of Physics, University of California, Berkeley, California 94720*

²*Material Sciences Division, Ernest Orlando Lawrence Berkeley National Laboratory, Berkeley, California 94720*

³*Advanced Light Source, Ernest Orlando Lawrence Berkeley National Laboratory, Berkeley, California 94720*

⁴*Center for Beam Physics, Accelerator and Fusion Research Division, Ernest Orlando Lawrence Berkeley National Laboratory, Berkeley, California 94720*

⁵*Institute of Physics and Astronomy, University of Aarhus, Ny Munkegade, DK-8000, Aarhus C, Denmark*

(Received 23 July 1998)

Ultrafast structural dynamics in laser-perturbed InSb are studied using time-resolved x-ray diffraction with a novel femtosecond x-ray source. We report the first observation of a delay in the onset of lattice expansion, which we attribute to energy relaxation processes and lattice strain propagation. In addition, we observe direct indications of ultrafast disordering on a subpicosecond time scale.

PACS numbers: 65.70.+y, 61.10.-i, 61.66.Dk, 64.60.-i

Because of the direct relationship between x-ray diffraction and crystal structure, time-resolved x-ray diffraction using femtosecond x-ray pulses is an attractive means of studying ultrafast structural dynamics in crystals [1]. While previous optical studies of Si [2,3], GaAs [4], and InSb [5] under high-intensity laser excitation have suggested that ultrafast disordering can occur, only *indirect* information about ultrafast structural dynamics was obtained. This is due to the indirect relationship between the optical and structural properties of crystals. To better study ultrafast structural dynamics in laser perturbed InSb, we utilize x-ray diffraction techniques on a femtosecond time scale using a novel femtosecond x-ray source based on Thomson scattering [6,7]. The x-ray diffraction measurements reveal a delayed onset and propagation of lattice expansion, and provide direct indications of structural disordering on a femtosecond time scale.

Time-resolved x-ray diffraction with femtosecond x-ray pulses (0.4 Å, 300 fs, 5 Hz) [6,7] is used to probe structural dynamics in InSb initiated by ultrashort laser pulses (800 nm, 100 fs). The InSb crystal is cut 3° off the (111) orientation to allow x rays to be diffracted by the (111) planes in the asymmetric Bragg geometry (the x-ray beam is incident ~0.4° relative to the crystal surface). This geometry provides a better match between the absorption depths (normal to the surface) of the x rays (~500 nm) and the laser light (~100 nm). A fraction (10%) of the x-ray generating laser beam is split off and used for sample excitation. The angle between the laser excitation beam (pump) and the x-ray beam (probe) is kept small (~4°) to reduce the temporal walkoff (~500 fs) between the beams. The temporal zero between the pump and probe pulses is determined to within ±300 fs by using a beam splitter to direct part of the x-ray generating laser beam along the probe beam path and cross-correlating this beam with the pump beam. The *p*-polarized laser beam illuminates an elliptical spot on the sample (about twice

the area of the x-ray beam) at a fluence of 20 mJ/cm² (below the single-shot damage threshold [5]). The sample is moved after multiple (~10⁴) laser shots. While slight surface damage (apparently recrystallized material mixed with amorphous material) occurs after multiple shots, no significant degradation in the x-ray diffraction signal is observed. Only the *reversible* changes in the sample are probed in our experiment. The x-ray beam is apertured to ~200 μrad in the diffraction plane to both increase the spectral resolution and decrease the diffracted photon count rate to about one every 10 x-ray pulses. This decreased count rate permits the diffracted energy spectrum to be obtained by pulse-height analysis using a LN₂ cooled Ge detector (~300 eV resolution at 30 keV). Data are collected by repeated cycling through a sequence of time delays, with data from 100 x-ray pulses accumulated per time delay on each cycle.

Representative diffraction spectra using 30 keV x rays (averaged over ~2 × 10⁴ x-ray pulses) for -20 and +100 ps time delays (positive time delays correspond to x-ray pulses arriving after laser pulses) are shown in Fig. 1. The peak of the spectrum at +100 ps is shifted by ~30 eV towards lower energy relative to the spectrum at -20 ps. This spectral shift is on the order of the shift (~80 eV) estimated for InSb uniformly heated to the melting temperature (803 K), with the lattice expansion (~9 × 10⁻³ Å per plane) determined by the thermal expansion coefficient (5 × 10⁶ K⁻¹ [8]). Since expanded lattice planes diffract lower photon energy x rays at a given incident angle, the spectral shift provides evidence that lattice expansion occurs on this time scale. Similar laser-induced lattice expansion has been observed in Si [9], and more recently in Au [10] and GaAs [11]. In addition to the spectral peak shift, the spectrum at +100 ps is broader than the spectrum at -20 ps. This broadening is a consequence of x rays diffracting from both expanded and unperturbed lattice planes, which can occur because the absorption depth for 30 keV x rays

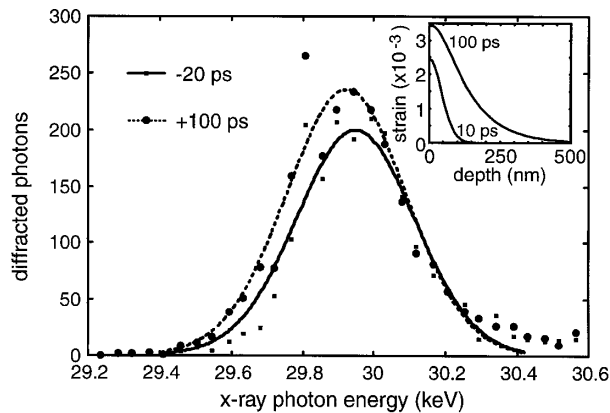
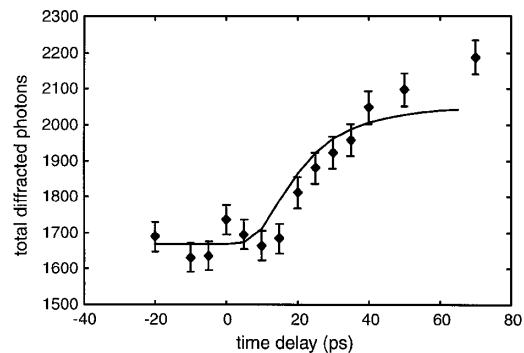


FIG. 1. Diffraction spectra from the laser perturbed InSb at time delays of -20 ps and $+100$ ps measured with 30 -keV, 300 -fs x-ray pulses. The curves are simulated x-ray diffraction profiles (from the model described in the text) convolved with the resolution of the Ge detector. Inset: Calculated strain profiles ($\Delta d/d$) at $+10$ ps (solid) and $+100$ ps (dashed).

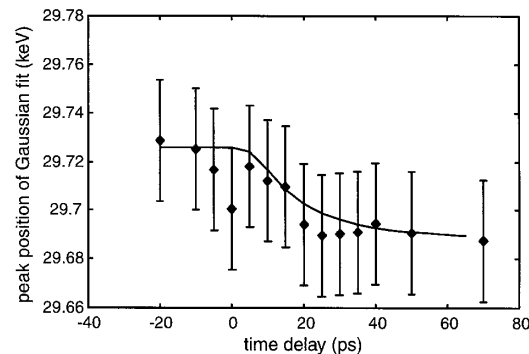
is large relative to the attenuation depth due to Bragg diffraction. Thus, lower-energy x rays from our collimated and polychromatic ($\Delta\lambda/\lambda \sim 15\%$) x-ray source [6] are diffracted by the layer of expanded lattice planes, while higher-energy x rays pass through the expanded layer (with negligible attenuation) and are diffracted by the underlying unperturbed lattice planes. Therefore, both the spectral shift and the integrated spectrum of diffracted x rays as a function of time delay provide quantitative information about lattice expansion dynamics.

Data representing the lattice expansion dynamics in InSb are shown in Fig. 2. Figure 2(a) shows the x-ray diffraction spectra integrated over the Bragg peak as a function of time delay. The rate of increase in the diffraction signal is consistent with a layer of strain ($\Delta d/d$, where d is the unperturbed lattice spacing) that increases in thickness at the speed of sound (5×10^5 cm/s [8]). An interesting delay (~ 10 ps) in the onset of lattice expansion is also observed. Such a delay has been suggested [4], but to our knowledge has not been previously observed. Figure 2(b) shows the corresponding spectral position of the Bragg peak as a function of time delay. The evolution of the spectral peak position provides further evidence of strain propagating at the speed of sound.

The nonequilibrium laser heating dynamics responsible for the observed lattice expansion behavior involve both carrier and phonon dynamics. Let us first consider the carrier dynamics, which we model following Ref. [12]. The absorbed laser pulse energy creates a dense electron-hole plasma ($\sim 4 \times 10^{21}$ carriers/cm³) with large excess energy (due to the small band gap of InSb), which quickly thermalizes (~ 100 fs) via carrier-carrier scattering [13]. This electron-hole plasma remains dense for a relatively long time (~ 1 ps), mainly because ambipolar diffusion partially offsets hot-carrier transport [14]. Because of the high-carrier density, Auger recombination is the domi-



(a)



(b)

FIG. 2. (a) Diffracted x-ray photons integrated over the Bragg peak and (b) spectral peak position as a function of time delay compared to the laser heated InSb simulation (solid lines) described in the text.

nant carrier recombination mechanism (radiative recombination is negligible for time scales < 1 ns), resulting in a lowering of the carrier density while maintaining the energy content in the plasma. The carrier energy is eventually transferred to the lattice through the emission of longitudinal-optical (LO) phonons. This is the dominant mechanism for carrier energy relaxation in zinc-blende materials, due to the strong Fröhlich coupling [15]. While the LO phonon emission time is ~ 200 fs, the large number of phonon emissions (~ 50 meV) needed to reduce the carrier energy (~ 1 eV) makes the effective energy relaxation time longer (~ 2 ps) [15,16].

The transfer of energy to the lattice leaves the lattice in a highly stressed state, which is eventually relieved by undergoing thermal expansion. If one assumes that the lattice vibrational modes are immediately thermalized upon energy transfer from the carriers, then the strain profile can be calculated using the resulting lattice temperature profile and the thermal expansion coefficient. Alternatively, the strain profile can be calculated directly from the LO phonon distribution via the appropriate mode Grüneisen parameters. However, the x-ray diffraction response calculated (using the strained crystal method in Ref. [9]) from the strain profile obtained in either fashion exhibits an onset of lattice expansion well before the observed onset.

Assuming a longer relaxation time between the carriers and the lattice merely reduces the overall strain and slows the rate of increase of the x-ray diffraction signal, but does not reproduce the observed delay. Thus, the phonon dynamics following carrier energy relaxation are intimately involved in the evolution of the lattice expansion dynamics.

The delay in the onset of lattice expansion is a signature of the nonequilibrium phonon dynamics that occur following carrier energy relaxation. As the population of LO phonons increases via energy transfer from the carriers, the atoms undergo increasingly anharmonic motion. This anharmonicity couples the LO phonons to acoustic phonons [17], eventually leading to local thermal equilibrium. However, energy transferred to phonons beneath the surface does not immediately cause lattice expansion because of confinement by the surrounding unperturbed crystal, leaving the heated layer in a highly stressed state. Because the surface is free to move, lattice expansion nucleates at the surface to relieve this stress, forming a highly strained layer. The large amount of stress in the underlying heated layer is relieved by propagation of strain from the surface, with the lattice expansion occurring primarily normal to the surface due to lateral confinement [18]. This strain propagation occurs via acoustic phonon propagation (diffusive thermal transport is too slow to account for strain propagation), which is quasiballistic (i.e., on the order of the speed of sound) under highly nonequilibrium conditions [19]. As LO phonons continue to decay into acoustic phonons, lattice expansion moves deeper into the sample.

To extract the essential physics, the phonon dynamics described above are modeled using a lattice equilibration time and an effective temperature profile. A single time constant is used to describe the energy transfer from the LO phonon population to a lattice in local thermal equilibrium. We estimate this time constant to be ~ 7 ps, based on recent optical dielectric constant measurements in GaAs near the ultrafast disordering threshold [4]. By assuming the lattice is locally in thermal equilibrium, the heat capacity can be used to calculate the lattice temperature profile. While the lattice temperature profile properly accounts for the energy in the lattice, it cannot be used to directly calculate lattice expansion because strain must nucleate at the surface and propagate inward. In order to simulate the nucleation and propagation of strain, an effective temperature profile is used to determine the evolving strain profile. This effective temperature profile is simply the lattice temperature profile multiplied by a Gaussian function that increases in width with time. The width of the Gaussian function in x ($x = 0$ at the surface) increases at the speed of sound, to account for ballistic transport of acoustic phonons. The strain profile is derived from the effective temperature profile via the thermal expansion coefficient.

Calculated strain profiles (using a 2 ps LO phonon emission time and a 7 ps acoustic phonon generation and

lattice equilibration time) are shown in the inset of Fig. 1. Using these strain profiles, the x-ray diffraction response is calculated (accounting for our x-ray source parameters and the Ge detector energy resolution) following the method in Ref. [9]. The calculated x-ray diffraction spectra (Figs. 1 and 3) and x-ray diffraction time evolution (Fig. 2) are in good agreement with the data. Our model indicates that the time delay in the onset of lattice expansion is determined primarily by the combination of LO phonon generation/relaxation times and propagation of lattice expansion. Screening during Auger recombination (which is important at carrier densities exceeding $\sim 10^{21}$ carriers/cm³) [20], and LO phonon reabsorption by carriers are secondary factors that may affect the delay.

On the femtosecond time scale, optical studies [3–5] and recent x-ray studies [21] suggest that exciting high-carrier densities ($\sim 10^{22}$ /cm²) in semiconductors can give rise to ultrafast (nonthermal) disordering. Ultrafast disordering is distinct from thermal melting because disordering occurs before a significant amount of energy can be transferred to the lattice by conventional electron-phonon interactions [22,23]. Below the single-shot damage threshold, ultrafast disordering is expected to occur only in a very thin layer (~ 10 nm). The data obtained using 30 keV x rays shows little evidence of such disordering, due to negligible absorption in the thin disordered layer. To properly investigate ultrafast disordering, the x-ray probing depth must be reduced to better match the disordering depth. In addition, the reduction of the x-ray probing depth permits the study of lattice expansion dynamics with reduced effects of strain propagation on the x-ray diffraction response. To obtain better matching between the laser and x-ray penetration depths, x-ray pulses with 7.3 keV photon energy are generated via Thomson scattering of laser pulses by 25 MeV electron bunches (instead of 50 MeV [6,7]). The resulting x-ray pulses (~ 500 fs duration) are used to perform time-resolved x-ray diffraction on an InSb crystal cut 12.8° off the (111) orientation. Under this asymmetric Bragg diffraction geometry, the x-ray probing depth (~ 50 nm) is better matched to the expected thin disordered layer. The laser excitation conditions are very similar to those for the 30 keV x-ray diffraction geometry previously described.

Figure 3 shows time-resolved x-ray diffraction data taken using 7.3 keV x-ray photons. Indications of a rapid decrease (< 1 ps delay) in the number of diffracted photons and a shift (+10 ps) in the diffraction peak are observed. The rapid decrease ($\sim 6\%$) in diffracted photons [Fig. 3(a)] is consistent with x-ray absorption and lack of Bragg diffraction in a disordered layer (~ 30 Å thick) that forms on a subpicosecond time scale. Disorder on this time scale is electronically induced, as the time scale for significant energy transfer from carriers to phonons is greater than 1 ps. Since no spectral shift of the diffraction peak is observed (within our experimental resolution) before 2 ps, the rapid decrease does not involve lattice expansion. The observed spectral

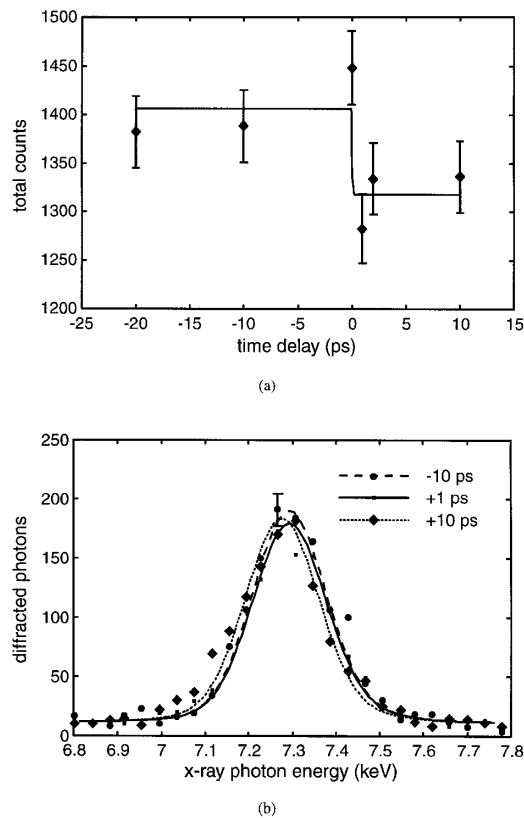


FIG. 3. (a) Normalized integrated x-ray diffracted photons as a function of time delay and (b) representative x-ray diffraction spectra (with simulated profiles) for different time delays, taken with 7.3-keV x rays.

shift without broadening at +10 ps [Fig. 3(b)] indicates that the strain is approximately uniform over the depth probed by the x rays. This shift is reproduced by our calculations (based on the strain profile shown in the inset of Fig. 1), and is consistent with the data shown in Fig. 2 (using 30 keV x rays). Here, we are more clearly observing the delayed onset in lattice expansion in the probed volume. While strain propagation still plays a role (~ 10 ps for sound propagation across 50 nm), it is evident that no significant lattice expansion occurs in less than 2 ps.

In summary, ultrafast structural dynamics in laser perturbed InSb are directly investigated using a novel femtosecond x-ray source. Lattice expansion on the picosecond time scale in the [111] direction (maximum increase of $\sim 10^{-2}$ Å per lattice plane) is evidenced in the x-ray diffraction spectrum by either a broadening (using 30 keV x rays) or by a spectral shift (using 7.3-keV x rays). We report the first direct observation of a ~ 10 ps delay in the onset of lattice expansion, which

we attribute to the combination of energy relaxation processes and strain propagation. The thickness of the lattice expansion layer is observed to increase at the speed of sound, as strain is relieved by acoustic phonon propagation from the surface into the crystal. At very early times (< 1 ps), we observe direct evidence of nonthermal ultrafast disordering of a ~ 30 Å surface layer caused by the formation of a dense electron hole plasma.

This work was supported by the U.S. Department of Energy under Contract No. AC03-76SF00098 and by the National Science Foundation under Grant No. PHY-9512693. The authors wish to acknowledge H.H.W. Chong for his help with data collection and T. Byrne and the Advanced Light Source operations crew for their technical support. A. H. C. would like to thank Dr. J. Larsson, A.M. Lindenberg, Professor R. W. Falcone, and Dr. T. Guo for enlightening discussions and J.K. Chin for his help with the simulations. P. B. gratefully acknowledges the support of the Carlsberg Foundation.

*Present address: W.W. Hansen Experimental Physics Laboratory, Stanford University, Stanford, California 94305.

- [1] C. Rischel *et al.*, *Nature (London)* **390**, 490 (1997).
- [2] C. V. Shank *et al.*, *Phys. Rev. Lett.* **50**, 454 (1983).
- [3] C. V. Shank *et al.*, *Phys. Rev. Lett.* **51**, 900 (1983).
- [4] L. Huang *et al.*, *Phys. Rev. Lett.* **80**, 185 (1998).
- [5] I.L. Shumay and U. Höfer, *Phys. Rev. B* **53**, 15 878 (1996).
- [6] R. W. Schoenlein *et al.*, *Science* **274**, 236 (1996).
- [7] W. P. Leemans *et al.*, *Phys. Rev. Lett.* **77**, 4182 (1996).
- [8] *American Institute of Physics Handbook*, edited by D. E. Gray (McGraw-Hill, New York, 1972).
- [9] B. C. Larson *et al.*, *J. Mater. Res.* **1**, 144 (1986).
- [10] P. Chen *et al.*, *J. Chem. Phys.* **104**, 10 001 (1996).
- [11] C. Rose-Petruck *et al.*, *Nature* **398**, 310 (1999).
- [12] A. Lietoila and J. F. Gibbons, *Appl. Phys. Lett.* **40**, 624 (1982).
- [13] T. Elsaesser *et al.*, *Phys. Rev. Lett.* **66**, 1757 (1991).
- [14] H. M. v. Driel, *Phys. Rev. B* **35**, 8166 (1987).
- [15] J. A. Kash *et al.*, *Phys. Rev. Lett.* **54**, 2151 (1985).
- [16] P. Langot *et al.*, *Phys. Rev. B* **54**, 14 487 (1996).
- [17] J. M. Ziman, *Principles of the Theory of Solids* (Cambridge University Press, Cambridge, MA, 1972).
- [18] S. Kojima *et al.*, *Jpn. J. Appl. Phys.* **33**, 5612 (1994).
- [19] R. G. Ulbrich *et al.*, *Phys. Rev. Lett.* **45**, 1432 (1980).
- [20] E. J. Yoffa, *Phys. Rev. B* **21**, 2415 (1980).
- [21] J. Larsson *et al.*, *Appl. Phys. A* **66**, 587 (1998).
- [22] P. L. Silvestrelli *et al.*, *Phys. Rev. Lett.* **77**, 3149 (1996).
- [23] P. Stampfli and K. H. Bennemann, *Appl. Phys. A* **60**, 191 (1995).